STEBS: Spatio-Temporal Entropy-Based Scoring Handover Model for LEO Satellite

Mohammad A. Massad
School of Computing
Queen's University
Kingston, ON, Canada
m.massad@queensu.ca

Abdallah Y. Alma'aitah
Department of Network Engineering and Security
University of Science and Technology
Irbid, Jordan
ayalmaaitah@just.edu.jo

Hossam S. Hassanein
School of Computing
Queen's University
Kingston, ON, Canada
hossam@cs.queensu.ca

Abstract—In 6G and beyond network infrastructure, Low Earth Orbit (LEO)-based Non-terrestrial Networks (NTN) are poised to play a significant role in delivering global connectivity. To serve users effectively, multiple satellites must collaborate. Each satellite has only a brief window of time to communicate with the user. Therefore, an optimal handover strategy is needed to ensure seamless user transitions between satellites while minimizing unnecessary and frequent handovers, which leads to user satisfaction. However, existing handover strategies, primarily based on system geometry, may lack efficiency in dynamically changing user demand, particularly in deep urban canyon environments. This paper introduces a Spatio-temporal Entropy-based Scoring (STEBS) handover strategy. STEBS is a multi-objective dynamic handover strategy designed to minimize the number of handovers while consistently meeting user demand. Simulation results demonstrate that STEBS reduces the number of handovers and increases throughput, achieving an exceptionally low blocking rate of one-eighth compared to benchmark schemes, resulting in a 99% user satisfaction rate.

Index Terms—LEO satellite, handover, channel model, entropy

I. Introduction

Satellite communications are seen as essential additions to the future 6G wireless network infrastructure, given their capacity to enhance the existing terrestrial communication network and deliver global wireless coverage [1], [2]. Recently, there has been increased research interest in Low Earth Orbit (LEO) satellite communications, which offer advantages such as decreased transmission loss, shorter delays, and lower power consumption compared to Geostationary Earth Orbit (GEO) satellite communications [3]–[5]. In terms of coverage, a single LEO satellite can span a vast diameter, covering hundreds of kilometers. The orbital dynamics of LEO satellite constellations, coupled with sky-to-ground propagation characteristics present link-level and network-level challenges not encountered in current terrestrial cellular networks. The success of emerging LEO satellite communication systems and their role in next-generation connectivity will depend on identifying potential solutions to these challenges.

One of the primary challenges facing LEO satellite communication systems is their high mobility, with speeds reaching 27,000 km/h, resulting in short coverage duration per satellite. Mobile terminals must disconnect from the currently linked satellite to maintain network sessions and establish a new connection with the next satellite. This process is known as satellite handover. This constant change in the connection relationship between satellites and terminals is necessary. However, satellite handovers can introduce issues, such as delays, transmission losses, and signaling overhead. Therefore, designing an intelligent satellite handover strategy that minimizes the average number of satellite handovers, enhances call quality, and balances network loads is of utmost importance.

The challenge of satellite handovers in Non-terrestrial Networks (NTN) is a prominent topic in academic research and industry. For instance, Duan et al. [6] introduced a handover control strategy that integrates multi-hop routing based on a minimum delay strategy with the option given to the satellite to decide the user access. Bukhari et al. [7] employed a fuzzy c-mean clustering approach for LEO satellite handover but did not consider call quality. Hu et al. [8] suggested a velocity-aware handover prediction in LEO satellite communication networks by capturing the impact of user mobility to avoid handover prediction failure.

Dai et al. [9] decomposed the optimization problem into the throughput maximization factor and the load balancing factor. They combined these factors to create a new metric and employed the Particle Swarm Optimization (PSO) algorithm to maximize this metric, thereby obtaining the optimal handover decision. Liu et al. [10] suggested a load-balanced satellite handover strategy, considering the equilibrium of satellite workloads. This strategy also integrates a power allocation optimization algorithm to enhance channel capacity.

Lei et al. [11] formulated a handover strategy for aircraft, incorporating dynamic user preferences specifically tailored for LEO satellite communication. Cao et al. [12] introduced user equipment (UE)-driven deep reinforcement learning (DRL)-based approach designed for random mobile ground terminals. The goal is to maximize the average system throughput while minimizing the handover rate. However, it is worth noting that their method does not consider system load balancing. Feng et al. [13]

presented a handover strategy based on bipartite graphs, utilizing the Kuhn-Munkres algorithm to match ground stations and satellites. The objective is to maximize communication quality and achieve a balanced satellite load distribution. However, most of the above handover strategies did not consider the users' dynamic service level agreement (SLA) or the deep urban canyon environment.

This paper proposes a spatio-temporal entropy-based scoring (STEBS) handover algorithm. STEBS is a multi-objective handover strategy based on a scoring mechanism within a satellite ground link. To evaluate the STEBS handover algorithm, we will compare it with the three performance criteria for satellite handovers: the remaining visible time, the elevation angle, and the available resources of the satellite. The remaining visible time directly influences the satellite handover rate. Ensuring a reasonable elevation angle during the communication contributes to maintaining call quality. The availability of satellite resources plays a role in determining the network load on the satellite. Additional evaluation criteria can be derived from these three fundamental criteria.

The rest of this paper is organized as follows. Section II presents the system model, offering a detailed overview of the channel model, handover procedure, problem formulation, and the STEBS model. Section III contains a thorough performance evaluation derived from our simulation results. Future research topics and the conclusion are presented in Section IV.

II. System Model

A. Channel Model

This paper utilizes a conventional geometric 3D multiple-input multiple-output (MIMO) channel model to establish downlink communication from a satellite to a user. The channel characteristics are delineated by describing the geometric interplay between scatterers and the transceiver within the propagation environment. The model assumes that the handover from a LEO satellite is similar to an inter-satellite handover, and the channel communication is established prior to the handover.

This study focuses on deep urban canyon areas as the model's setting, characterized by dense scatterers such as trees and tall buildings with narrow roads, as depicted in Figure 1. Consequently, the probability of encountering non-line-of-sight (NLOS) conditions are notably high around the user terminal, and terminal scatterers are distributed across the 3D hemisphere surface.

The overall path loss is assumed to comprise free-space path loss (FSPL) and atmospheric absorption, accounting for oxygen (α_{O2}) and water vapor (α_{H2O}) attenuation during propagation from the satellite to the user [14]. Other types of gases, however, have a negligible effect on changing the signal level for elevation angles above 30° [15]. The satellite altitude is denoted as h_s, while the horizontal distance between user u and satellite s is represented by $d_{u,s}$. The elevation angle between the user equipment antenna array direction and the x-axis is denoted as $\phi_{u,s}$

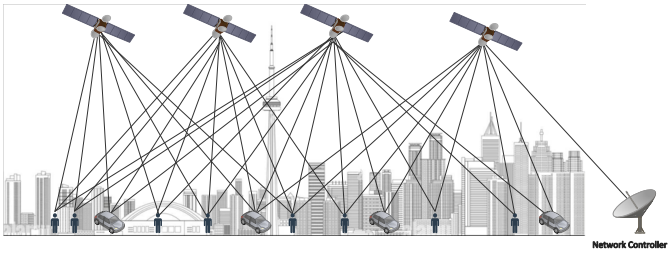

Fig. 1: System Model

The 3D channel model proposed for deep urban canyons can be articulated as follows:

$$PL_{total} = FSPL + \Theta \tag{1}$$

where PL_{total} is the total path loss between the satellite s and user u, $FSPL$ is the free space air-to-ground path loss and Θ is the atmospheric absorption and calculated as,

$$\Theta = \alpha.d \tag{2}$$

where α is the specific attenuation due to atmospheric gases (in dB/km), and d is the path distance through the atmosphere (in km).

1) Free Space Air-to-Ground Path Loss: An important aspect of the air-to-ground channel is the probability of Line-of-Sight (LOS) connectivity. The modeling of the probability for the LOS channel between the satellite and the user is presented as follows [16]–[18]:

$$P_{LoS} = \frac{1}{1 + a.exp(-b(\frac{180}{\pi}\arctan(\frac{h_s}{d_{s,u}})) - a)} \tag{3}$$

where a and b are constants depending on the environment model.

Therefore, the probability of NLOS is,

$$P_{NLos} = 1 - P_{LoS} \tag{4}$$

The slant distance between satellite s and user u is represented by $d_{s,u}$, and defined in relation to the satellite's altitude h_s and its elevation angle ϕ as in Equation 5,

$$d_{s,u} = \sqrt{R_e^2 sin^2\phi + h_s^2 + 2R_e h_s} - R_e sin\phi_{u,s} \tag{5}$$

where R_e is the Earth radius, $\phi_{u,s}$ is the Elevation Angle (EV). Considering air-to-ground channel in deep urban canyon environments. where multi-path fading and shadowing exist then the path loss for LOS and NLOS is modeled as the following,

$$PL_{LoS} = 20log(\frac{4\pi f_c d_{ik}}{c}) + \eta LoS \tag{6}$$

$$PL_{NLoS} = 20log(\frac{4\pi f_c d_{ik}}{c}) + \eta NLoS \quad (7)$$

Therefore, the free space path loss ($FSPL$) is modeled as,

$$FSPL = P_{LoS}.PL_{LoS} + P_{NLoS}.PL_{NLoS} \quad (8)$$

Substituting (3), (4) and (6) into (7), $FSPL$ is presented as:

$$FSPL = \frac{A}{1 + a.exp(-b(\frac{180}{\pi}\arctan(\frac{h_s}{d_{s,u}})) - a)} + 10log(h_s^2 + r_{ik}^2) + B \quad (9)$$

where $A = \eta LoS - \eta NLoS$ and $B = 20log(\frac{4\pi f_c}{c}) + \eta NLoS$ are the path loss exponent for ηLOS and ηNLOS.

2) Atmospheric Absorption: The atmospheric absorption accounts for oxygen (α_{O2}) and water vapor (α_{H2O}) attenuation during propagation [14]

$$\alpha = \alpha_{O2} + \alpha_{H2O} \quad (10)$$

Under an environment with additive Gaussian white noise, the received Signal-to-Noise Ratio (SNR) of user u can be measured in dB:

$$SNR(h_s, d_{s,u}) = P_t - P_n - PL_{total}(h_s, d_{s,u}) \quad (11)$$

where P_t and P_n are the transmission power and average power of noise in dBm respectively and the available data rate can be calculated as,

$$DR_{s,u} = BW \cdot log(1 + SNR(h_s, d_{s,u})) \quad (12)$$

B. Handover Procedure

This section introduces the data rate-based event-triggering procedure. The handover model aligns with the methodology proposed in [19], [20], given its capability for autonomous decision-making and its utilization of a trigger-based handover process, analogous to the conventional handover process employed in the 3GPP New Radio (NR), as depicted in Figure 2. The figure outlines the handover procedure, integrating a data rate-based measurement report that acts as the trigger for initiating the handover process. If the data rate $DR_{s,u}$ delivered from satellite s to user u falls below the minimum user SLA threshold $DR_{u,sla}$, a handover will be triggered,

$$DR_{s,u} < DR_{u,sla}$$

As introduced in Figure 2, if the data rate condition is satisfied, , then the following steps are:

1) UE sends the measured data to the serving satellite;
2) Serving satellite transmits data to the network controller;

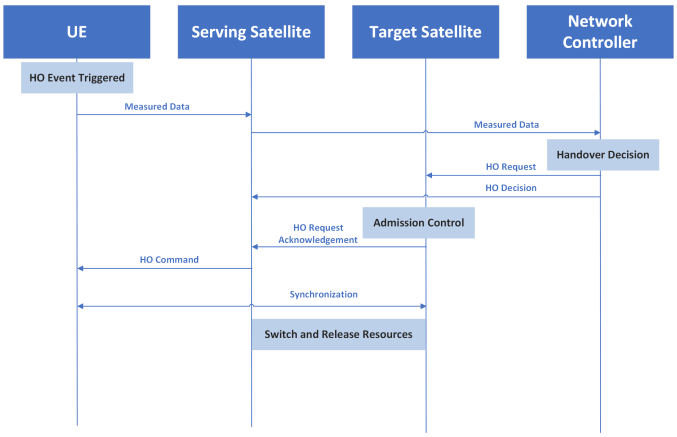

Fig. 2: Handover Procedure

3) Upon receiving the measured data, the network controller decides to initiate the handover;
4) The network controller sends the handover request and decision to the target and serving satellites;
5) Targeted satellite exchanges the handover request acknowledgment message with the serving satellite;
6) Serving satellite sends the handover command to the corresponding UE;
7) UE synchronizes its data with the target satellite;
8) UE switches the communication route to the target satellite; and
9) UE disconnects from the serving satellite and releases its resources.

C. Satellite Scoring Model

In this part of the process, the available satellite for each user will be weighted. While the output of this process is the scoring metric that gives a user preference for each satellite, the input is three metrics: Available Resources (AR), Remaining Time (RT) and available Data Rate (DR). Since each metric has a different level of importance in determining the overall satellite score based on its data, assigning weights to each metric is essential since it allows the scoring function to express each metric's relative importance or contribution to the overall score. In such a scenario, introducing weights can control the influence of each metric on the final score.

1) Weight Calculation: We will use entropy from information theory to assign weight to each metric. Following the fundamental principles of information theory, information serves as a quantification of the certainty or order in a system, while entropy is a measure of uncertainty or randomness associated with a dataset. It quantifies the amount of information contained in a dataset. Introduced by Claude Shannon, entropy provides a way to characterize the average unpredictability in a set of possible outcomes.

Therefore, the general formula of information entropy for user u on metric m is:

$$E_{u,m_j} = -\sum_{i=1}^{n} P_i \log_2 P_i \tag{13}$$

where P_i is the probability of the i^{th} element in the metric m_j for user u.

To determine the weight of each metric m_j for user u, given their disparate units (e.g., time, Mbps, and number of channels), and acknowledging that minimal differences within the same metric are negligible in the overall evaluation, we will utilize the KMeans clustering algorithm to dynamically group values within each metric. This clustering aims to standardize their representation before entropy calculation. The optimal number of clusters (optimal K) for each metric is determined through elbow gap statistics.

After clustering the four metrics, the subsequent step involves calculating the entropy for each, as outlined in Equation 13. The weight of each row in each metric is then computed according to Equation 14.

$$w_{u,m_j} = \frac{E_{u,m_j}}{\sum_1^m E_{u,m_j}} \tag{14}$$

where w_{u,m_j} represents the assigned weight for user u in metric m_j.

2) Satellite Scoring: Once we assigned a weight for each metric, we will calculate the score of all available satellites to each user u as in Utility Function 15

$$Score_{u_i}^{s_j} = w_{rt} RT_{u_i,s_j} + w_{dr} DR_{u_i,s_j} + w_{ar}(1 - U_{s_j}) \tag{15}$$

where, $Score_{u_i}^{s_j}$ is the satellite s_j preference score for user u_i, w_{rt}, w_{dr}, w_{ar} is the assigned weight for metric RT, DR, and AR respectively, and U_{s_j} is s_j satellite utilization.

RT_{u_i,s_j} and DR_{u_i,s_j} as in equations 16 and 17.

$$RT_{u_i,s_j} = \frac{RT_{u_i,s_j} - RT_{min}}{RT_{max} - RT_{min}} \tag{16}$$

$$DR_{u_i,s_j} = \frac{DR_{u_i,s_j} - DR_{u_i,s}^{min}}{DR_{u_i,s}^{max} - DR_{u_i,s}^{min}} \tag{17}$$

In Equation 16, the values RT_{min} and RT_{max} are reference values based on the LEO satellite's speed in its orbit, the environment, and the specific location being studied. Additionally, $DR_{u_i,s}^{min}$ and $DR_{u_i,s}^{max}$ represent the minimum and maximum acquired data rates for user u_i among all available satellites s at any given time.

3) Satellite Perfect Matching and Users Association: The input for this process consists of four metrics: satellite scoring, satellite available resources, users' SLA, and available data rate metrics.

To achieve the perfect matching, we will employ an Integer Linear Optimization. The problem formulation, objective function, and constraints are detailed in Section II-D.

D. Problem Formulation

The problem is formulated as a 0-1 integer linear program (0-1 ILP), utilizing the decision variable x_{u_i,s_j}, which is set to 1 if user u_i is assigned to satellite s_j, and 0 otherwise. The objective is to maximize the overall user score $Score_{u_i,s_j}$ and enhance user satisfaction. STEBS achieves this by maximizing the summation of the placement decision variable x_{u_i,s_j}. The optimization problem is given by 18.

$$\max \sum_{i=1}^{I} \sum_{j=1}^{J} x_{u_i,s_j} Score_{u_i,s_j} \tag{18a}$$

$$\text{s.t. C1: } DR_{min,u} \leq DR_{u,s}, \forall u \in U, \forall s \in S \tag{18b}$$

$$\text{C2: } DR_{max,u} \geq DR_{u,s}, \forall u \in U, \forall s \in S \tag{18c}$$

$$\text{C3: } \sum_{u=1}^{U} m \times l_{u,s} \leq L, \forall u \in U, \forall s \in S \tag{18d}$$

$$\text{C4: } Link_s^u \leq 1, \forall s \in S, \forall u \in U, \forall s \in S \tag{18e}$$

$$\text{C5: } \phi_{u,s} \geq \phi_0, \forall s \in S, \forall u \in U \tag{18f}$$

The optimization problem 18a aims to maximize the user score $Score_{u_i,s_j}$. Constraints (18b) and (18c) ensure that user u_i receives a data rate within their SLA profile's minimum and maximum limits; this is needed as user satisfaction is determined by the attained data rate compared to their SLA profile. However, given that each satellite has limited available channels L, assigning users based solely on maximizing the acquired data rate could negatively impact overall system performance. Additionally, in cases where no available link exists, user admission would fail.

To ensure that no satellite is overburdened with the number of assigned channels, constraint (18d) is introduced. Constraint (18d) guarantees that the sum of the number of assigned channels $n \times l$ for users in set U to any satellite s never exceeds the available resources on that satellite. Furthermore, as each user can only connect to one satellite at any given time constraint (18e) is included to govern this condition. Finally, since our target environment is an deep urban canyon where the probability of Line-Of-Sight (LOS) is very low, we introduce constraint (18f) to ensure that the acceptable elevation angle $\phi_{u,s}$ is greater than or equal to the minimum defined elevation angle.

E. STEBS Handover Algorithm

Due to the significant complexity of the proposed NP problem, solving it using exact dynamic programming remains largely theoretical [21]. Therefore, to address this optimization problem, the STEBS algorithm is introduced. The proposed handover strategy is encapsulated in Algorithm 1.

Lines 1-4 in Algorithm 1 involve collecting information about triggered users and their available satellites. The first loop of the STEBS algorithm (Lines 5-9) computes

Algorithm 1 STEBS Handover Algorithm

1: Find all UE U triggered for handover
2: Query users SLA $\forall u$
3: Find available satellite s $\forall u$
4: Query elevation angle ϕ and available resources AR $\forall s$
5: while $u \neq 0$ do
6: while $s \neq 0$ do
7: compute DR_{s_i,u_j} ▷ Eq. 12
8: $s - 1$
9: end while
10: $u - 1$
11: end while
12: for each Input metrics m do
13: Cluster DR metric
14: Cluster RT metric
15: Cluster AR metric
16: end for
17: for each Input metrics m do
18: for each u in m_i do
19: Calculate entropy E_{u,m_j} ▷ Eq. 13
20: Assign weight w_{u,m_j} based on E_{u,m_j} ▷ Eq. 14
21: end for
22: end for
23: while $u \neq 0$ do
24: for each Input available s do
25: Calculate $Score_{s_j}^{u_i}, \forall s$ ▷ Eq. 15
26: end for
27: $u - 1$
28: end while
29: Find perfect matching $\forall u \in U, \forall s \in S$
30: while $u \neq 0$ do
31: if u can connect to TN then
32: Connect to TN
33: else
34: Connect to assigned s
35: end if
36: $u - 1$
37: end while
38: Exit

the DR between each triggered user u and the available satellites. After DR computation, three metrics are prepared for use in satellite scoring. Lines 10-25 assign a score to each available satellite. For instance, Lines 10-14 standardize the units of the metrics and eliminate the minor differences inside the same metric by clustering them using the KMeans algorithm, as defined in Section II-C1. In Lines 15-20, the STEBS algorithm calculates the entropy for each metric m for each user u as in Equation 13 and assigns a weight based on the calculated entropy, as in Equation 14. The last part of the scoring function assigns a score for each available satellite to each user; this is done inside the loop defined in Lines 21-25, where the satellite score calculation is performed using the defined utility function in Equation 15.

Once STEBS assigns a score to each available satellite for each user, Line 26 finds the perfect matching using integer linear programming, as defined in Section II-D. Finally, Lines 27-33 aim to reduce the cost and load of connecting users to satellites. For instance, Line 28 checks if the user can connect to terrestrial networks (TN), given that the available TN can satisfy their SLA. If not, Line 31 connects the user to its assigned satellite.

III. Simulation Result and Discussion

In this section, we evaluate the performance of the STEBS handover strategy for satellite communication systems through a series of simulations. These simulations are conducted in the context of deep urban canyon environments characterized by dense user populations and elevated scatterers predominantly from tall buildings and scattered trees. Table I summarizes the parameters used in these simulations. Some parameters are set according to Starlink satellite specifications, while others align with LEO satellite development trends [22], [23]. Considering the urban canyon environment, it is reasonable to set high values for the path loss exponent A and B [24], and a minimum elevation angle ϕ_{min} to be high enough to maintain an acceptable LOS probability according to 3GPP Release 15 [25].

TABLE I: Simulation Parameters

Parameter	Description	Value
R_e	Earth Radius	6371 km
f_c	Frequency	10.7 GHz
h_s	Satellite Altitude	550 km
T	Noise Temperature	285 Kelvin
e	Vapor Pressure	9.36 hPa
P_t	Transmit Power	85.89 dbm
BW	Bandwidth	120 Mbps
A	LOS Path Loss Component	2.5 dB
B	NLOS Path Loss Component	20 dB
ϕ_{min}	Minimum Elevation Angle	20°

A. Simulation Setup

We implemented the STEBS, largest service time (max RT), largest data rate (max DR), least used satellite resources (max AR), and highest elevation angle (max EA) handover selection strategies using Python. We employed the PuLP optimization solver to address the diverse optimization problems. The dataset was generated through STK 17.1 by analyzing SpaceX Starlink satellite constellation coverage, as depicted in Table 3. The study area was covered by 10 LEO satellites at the selected time. However, not all of them provided the required data rate, especially when the elevation angle under 20°. Although the visible time of the satellites ranges between 491 to 756 seconds, the actual acceptable time, considering the data rate satisfaction range was significantly lower. The

generated dataset for this simulation includes the triggered users for handover set to 1000, facilitating the simulation of a group handover.

Access	Access Start	Access End	Duration (sec)	Higher Elevation (deg)	Min Rang (Km)	Max Rang (Km)
1	16:22:34	16:35:03	749	46.552	732.9135	2713.4291
2	16:23:20	16:31:31	491	6.239	2097.1347	2709.3326
3	16:20:50	16:31:40	650	15.381	1496.3006	2711.0974
4	16:25:55	16:38:38	763	74.291	570.1127	2713.6493
5	16:16:10	16:28:16	726	27.419	1059.9015	2713.5217
6	16:26:48	16:38:37	709	22.356	1212.7654	2712.2535
7	16:28:42	16:41:15	753	44.353	758.7964	2713.8254
8	16:14:24	16:24:46	622	13.243	1594.6204	2692.1841
9	16:27:03	16:39:39	756	75.306	560.0845	2694.9252
10	16:22:02	16:34:05	723	28.122	1029.2747	2694.9212

Fig. 3: Satellite Visible Time Report

Figures 4 and 5 provide a comparison of various handover strategies. This paper compares the STEBS algorithm with strategies based on max RT, max DR, max AR, and max EA.

For instance, in Figure 4, the left y-axis illustrates the average time between handovers. As depicted in the figure, the Max RT strategy outperforms the other strategies as it selects the next satellite with the largest service time. However, STEBS, which considers the remaining time when assigning a score to each satellite, exhibits slightly better results than the other strategies.

We conduct the same comparison regarding the average throughput per user. The right y-axis in Figure 4 presents the average throughput per user for the five different strategies, illustrating the throughput during the selected simulation snapshot time. Considering that throughput depends on both continuous transmission time and available data rate, once again, the Max RT strategy exhibits better results compared to the other methods. The STEBS strategy follows as the second-best, considering its incorporation of both available data rate and service time as part of the utility function parameters.

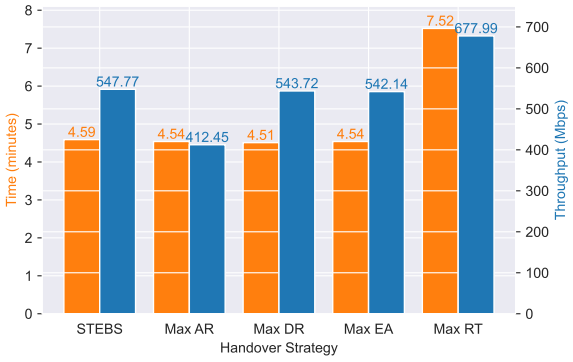

Fig. 4: Average Time Between Handovers and Average Throughput

While Figure 4 displays the average time between handovers and the average throughput per user, the left y-axis in Figure 5 illustrates the handover blocking rate, an important metric for measuring user Quality of Service (QoS). In this figure, we observe that the STEBS algorithm takes into consideration the fairness of service distribution among users. In our simulation, STEBS provides service for 99% of users, guaranteeing that each one of them will receive a data rate within their SLA ranges. The remaining 1% of users were blocked since there was no satellite with sufficient resources to guarantee users' SLAs, whereas the other methods had higher blocking rates.

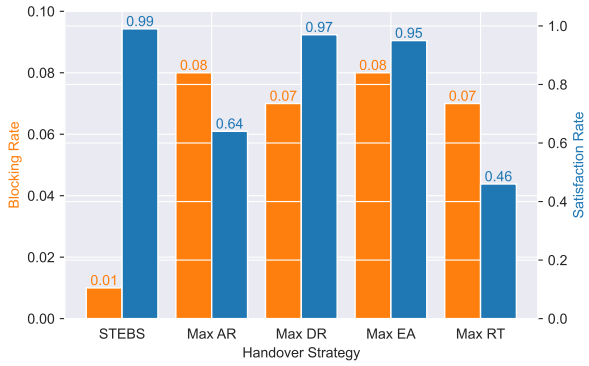

Fig. 5: Blocking Rate and Satisfaction Rate

A finally decisive benchmark is user satisfaction, measured by the data rate, the user receives relative to their SLA profile. User satisfaction rate ω is defined by Equation 19.

$$\lambda = \frac{DR_{u_i,s_j}}{SLA_{u_i}^{max}}$$

$$\omega = \begin{cases} 1 & \lambda >= SLA_{u_i}^{max} \\ \lambda & SLA_{u_i}^{min} < x < SLA_{u_i}^{max} \\ 0 & \lambda = SLA_{u_i}^{min} \end{cases} \quad (19)$$

While the maximum remaining time strategy outperforms in terms of total throughput and average time between handovers, the right y-axis in Figure 5 shows how it falls short in terms of user satisfaction. Compared to other strategies, the STEBS strategy prioritizes user satisfaction by including user fairness in assigning satellite scoring.

IV. Conclusion

In this study, we assessed the handover performance of a LEO-based NTN in an deep urban canyon environment, employing various handover strategies. Simulation findings reveal that the STEBS surpasses other strategies in terms of user satisfaction rate, minimal handover rate, and maximum throughput. Unlike existing techniques, STEBS introduces a multi-objective dynamic handover strategy utilizing a distinctive scoring method. In the future, a detailed comparison will be conducted to contrast

the STEBS algorithm with state of the art handover algorithms. In addition, as this method is implemented to work on a reactive-based strategy within a specific time slot, it has been suggested we explore the feasibility of implementing STEBS in a proactive-based strategy.

References

[1] Li, L., Chen, T., Wang, W., Song, X., You, L. and Gao, X., 2022. LoS MIMO transmission for LEO satellite communication systems. China Communications, 19(10), pp.180-193.

[2] Wang, W., Gao, L., Ding, R., Lei, J., You, L., Chan, C.A. and Gao, X., 2021. Resource efficiency optimization for robust beamforming in multi-beam satellite communications. IEEE Transactions on Vehicular Technology, 70(7), pp.6958-6968.

[3] Di, B., Song, L., Li, Y. and Poor, H.V., 2019. Ultra-dense LEO: Integration of satellite access networks into 5G and beyond. IEEE Wireless Communications, 26(2), pp.62-69.

[4] Li, K.X., You, L., Wang, J., Gao, X., Tsinos, C.G., Chatzinotas, S. and Ottersten, B., 2021. Downlink transmit design for massive MIMO LEO satellite communications. IEEE Transactions on Communications, 70(2), pp.1014-1028.

[5] You, L., Qiang, X., Tsinos, C.G., Liu, F., Wang, W., Gao, X. and Ottersten, B., 2022. Beam squint-aware integrated sensing and communications for hybrid massive MIMO LEO satellite systems. IEEE Journal on Selected Areas in Communications, 40(10), pp.2994-3009.

[6] C. Duan, J. Feng, H. Chang, B. Song, and Z. Xu, A novel handover control strategy combined with multi-hop routing in LEO satellite networks, in Proc. IEEE Int. Parallel Distrib. Process. Symp. Workshops (IPDPSW), May 2018, pp. 845–851.

[7] S. U. Bukhari, L. Yu, X. Q. Di, C. Chen, and X. Liu, Fuzzy C-mean clustering based: LEO satellite handover, in Proc. ICPCSEE, vol. 901, Sep. 2018, pp. 347–358.

[8] X. Hu, H. Song, S. Liu, and W. Wang, Velocity-aware handover prediction in LEO satellite communication networks, Int. J. Satell. Commun. Netw., vol. 36, no. 6, pp. 451–459, 2018.

[9] C. -Q. Dai, J. Xu, J. Wu and Q. Chen, "Multi-objective Intelligent Handover in Satellite-Terrestrial Integrated Networks," 2022 IEEE International Conference on Communications Workshops (ICC Workshops), Seoul, Korea, Republic of, 2022, pp. 367-372, doi: 10.1109/ICCWorkshops53468.2022.9814653.

[10] Liu Y, Feng L, Wu L, et al. Joint optimization based satellite handover strategy for LEO satellite networks. IET Commun. 2021; 15: 1576–1585. https://doi.org/10.1049/cmu2.12170.

[11] Y. H. Lei, L. F. Cao and M. Da Han, "A Handover Strategy Based on User Dynamic Preference for LEO Satellite," 2021 7th International Conference on Computer and Communications (ICCC), Chengdu, China, 2021, pp. 1925-1929, doi: 10.1109/ICCC54389.2021.9674431.

[12] Y. Cao, S. -Y. Lien and Y. -C. Liang, "Deep Reinforcement Learning For Multi-User Access Control in Non-Terrestrial Networks," in IEEE Transactions on Communications, vol. 69, no. 3, pp. 1605-1619, March 2021, doi: 10.1109/TCOMM.2020.3041347.

[13] L. Feng, Y. Liu, L. Wu, Z. Zhang and J. Dang, "A Satellite Handover Strategy Based on MIMO Technology in LEO Satellite Networks," in IEEE Communications Letters, vol. 24, no. 7, pp. 1505-1509, July 2020, doi: 10.1109/LCOMM.2020.2988043.

[14] Rosenkranz, Philip. "Absorption of microwaves by atmospheric gases." John Wiley and Sons, 1993.

[15] International Telecommunication Union. (2015). Recommendation ITU-R P.834-7: Effects of tropospheric refraction on radiowave propagation. ITU

[16] S. Naoumi et al., "Emergent Communication in Multi-Agent Reinforcement Learning for Flying Base Stations," 2023 IEEE International Mediterranean Conference on Communications and Networking (MeditCom), Dubrovnik, Croatia, 2023, pp. 133-138, doi: 10.1109/MeditCom58224.2023.10266608.

[17] E. Kim, I. P. Roberts and J. G. Andrews, "Downlink Analysis and Evaluation of Multi-Beam LEO Satellite Communication in Shadowed Rician Channels," in IEEE Transactions on Vehicular Technology, doi: 10.1109/TVT.2023.3312977.

[18] Z. Zhu, L. Li and W. Zhou, "QoS-aware 3D Deployment of UAV Base Stations," 2018 10th International Conference on Wireless Communications and Signal Processing (WCSP), Hangzhou, China, 2018, pp. 1-6, doi: 10.1109/WCSP.2018.8555923.

[19] Q. Kong, R. Lu and F. Yin, "Achieving Efficient and Secure Handover in LEO Constellation-Assisted Beyond 5G Networks," in IEEE Open Journal of the Communications Society, vol. 3, pp. 641-653, 2022, doi: 10.1109/OJCOMS.2021.3139462.

[20] J. -H. Lee, C. Park, S. Park and A. F. Molisch, "Handover Protocol Learning for LEO Satellite Networks: Access Delay and Collision Minimization," in IEEE Transactions on Wireless Communications, doi: 10.1109/TWC.2023.3342975.

[21] Y. He, B. Sheng, H. Yin, D. Yan and Y. Zhang, "Multi-objective deep reinforcement learning based time-frequency resource allocation for multi-beam satellite communications," in China Communications, vol. 19, no. 1, pp. 77-91, Jan. 2022, doi: 10.23919/JCC.2022.01.007.

[22] Space Exploration Holdings, LLC. (2018). Application for Fixed Satellite Service [SAT-MOD-20181108-00083]. Retrieved from FCC.report

[23] Z. Gao, A. Liu and X. Liang, "The Performance Analysis of Downlink NOMA in LEO Satellite Communication System," in IEEE Access, vol. 8, pp. 93723-93732, 2020, doi: 10.1109/ACCESS.2020.2995261.

[24] 3rd Generation Partnership Project (3GPP). (2021). Draft Technical Report and Technical Proposal 36.763 IoT NTN [RAN1-104e-R1-210XXXX]

[25] 3rd Generation Partnership Project (3GPP). (2020). Technical Specification Group Radio Access Network; Study on New Radio (NR) to support non-terrestrial networks